High Performance Inertial Navigation Grade Sigma-Delta MEMS Accelerometer

P. Zwahlen[1], Y. Dong[1], A-M. Nguyen[1], F. Rudolf[1], P. Ullah[2], V. Ragot[2]

[1] Colibrys SA
Maladière 83
2000 Neuchâtel
SWITZERLAND

[2] Sagem, Avionics Division
72-74, Rue de la Tour Billy
95101 Argenteuil
FRANCE

Inertial Sensors and Systems 2012
Karlsruhe, Germany

Abstract

In this paper, we report a Sigma-Delta MEMS navigation grade accelerometer, which, to our knowledge, is the first reported MEMS accelerometer to reach navigation grade performances. This reported system encompasses a high stability and high shock resistance mechanical MEMS sensor, a 5^{th}-order sigma-delta closed-loop electronic with digital loop filtering and high stability voltage reference.

Reported performances for a full scale range of 15g, with shock survivability up to 4000g, are a 10 μg bias stability under warm-up, a bias temperature slope below 200 μg/°C, a scale factor temperature slope below 100 ppm/°C, 2^{nd} order non-linearity below 20 $\mu g/g^2$ up to 1 kHz and a white noise floor below 2μg/√Hz.

The reported performances make this accelerometer of the same class as the traditional macro electro-mechanical quartz accelerometer.

1. Introduction

Inertial navigation grade accelerometer market has so far been captured by the macro electro-mechanical accelerometer [1] and quartz resonating accelerometers [2]. While the first ones reach high performances, they are expensive and fragile. The second ones have excellent dynamic range, but exhibit degraded stability performance and very low g-shock tolerance.

MEMS accelerometer technology has the potential to address these issues, as its batch manufacturing process makes their price cost attractive in volume quantities and their rugged assembly and low weight make them highly tolerant to high-g shock. Despite the market demand for a good MEMS alternative, there is to our knowledge no MEMS accelerometers that have been able to satisfy the high bias stability performance required for inertial navigation grade accelerometer. Commercial products satisfying to tactical grade performances are only now entering the market.

Bringing MEMS accelerometer towards inertial navigation grade level, significant design effort on bias stability is required. Compared to previous published work [3] [4], this design takes advantage of the extremely high mechanical stability of the MEMS accelerometer.

Compared to earlier published results [5] [6], we report significant progress on bias stability and temperature sensitivities through system optimization, thanks to in-depth understanding of the switched capacitive detection circuit and the electrostatic motor.

This article reviews in part II the key system design aspects that are instrumental in order to reach the highly demanding bias stability specifications to comply with inertial navigation

grade accelerometer. In part III, measurement results are presented, confirming that this reported MEMS accelerometer is fit for inertial navigation applications

2. System Design

2.1. Need for closed-loop operation

In order to address the navigation grade application performance requirements, the MEMS accelerometer has been embedded in a closed-loop regulation. The key drivers for operating in a servo loop configuration are described here below:

- ***Noise:*** mass damping does no more need to be achieved through gas, but through electronic regulation. For this reason mechanical Brownian noise can be significantly reduced [7].
- ***Vibration:*** Due to reduced mass excursion compared to open-loop accelerometer, non-linearity can be significantly lowered. Furthermore, thanks to operation at reduced gas, squeeze film effect is minimized.
- ***Signal bandwidth:*** closed-loop operation increases this bandwidth by 2 orders of magnitude compared to an open-loop operation. This is a key point for inertial navigation and guidance application, where the precision of the time stamp associated to a position data is essential.

2.2. Sigma-Delta architecture

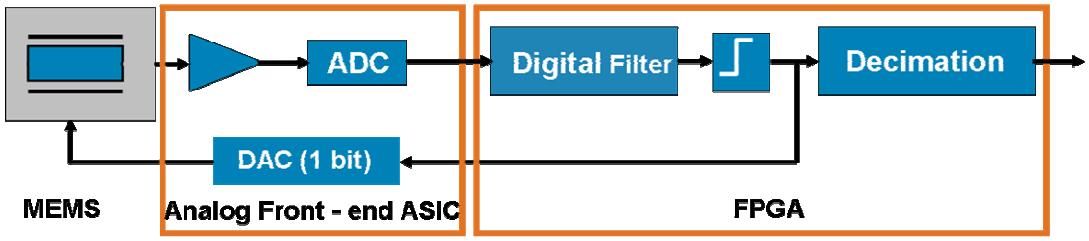

Figure 1: Sigma-Delta accelerometer close-loop architecture

The overall loop architecture depicted in Figure 1 is based on a 5th order Sigma-Delta regulation where the 2nd-order integrator accelerometer MEMS sensor is part of the loop. The MEMS sensor is based on bulk micromachining technology: its seismic mass, with out-of-plane displacement, is sandwiched between two fixed silicon electrodes. This 3-stack is assembled in a high temperature Silicon Fusion Bonding (SFB) process. The seismic mass position is captured through capacitive readout in a 7-bit low resolution switched capacitor voltage amplifier described in detail in [8]. This amplified signal is then digitalized in a 7-bits ADC, before being processed in the loop filter characterized by

infinite gain in low frequency (3rd-order integrator), inside an FPGA. This signal is then processed through a 1-bit sign comparator, which outputs the bitstream. This bitstream carries the acceleration signal information in a 1-bit format but at highly oversampled ratio, which after decimation, corresponds to a 24 bits SNR system in a 1 Hz frequency window. The signed 1-bit information coming out of the comparator is then fed back in a 1-bit DAC to generate an electrostatic actuation force pulse on the accelerometer MEMS sensor.

The choice for the implemented close-loop architecture based on a Sigma-Delta principle is particularly well adapted to MEMS accelerometer regulation as it brings the following key advantages:

- Sigma-Delta is well suited for low-frequency signals, which does correspond to the frequency band of acceleration signals. Noise shaping principle rejects quantization noise in high frequency bands.
- Sigma-Delta regulation is well adapted with time multiplexing concept. This allows the usage of the same electrodes for both sense readout and electrostatic force actuation.
- Simplicity of hardware implementation. Oversampling concept allows significant design relaxation of the analog detection chain signal resolution to only 7 bits. Additionally the voltage reference used for actuation force feedback is also of simple implementation as it is a 1-bit D/A converter, thus simplifying its design. It needs however to be emphasized that all these design relaxations come at the expense of increased system design complexity.
- Linearization of the electrostatic forces thanks to the Sigma-delta principle (through force averaging) furthermore reduces non-linearity overall and more importantly its even-order terms, which result in rectification error. Since inertial navigation mission are affected by important environmental vibrations, it is essential to keep Vibration Rectification Error (VRE) terms as small as possible.
- Sigma-Delta signal output is inherently a digital signal, thus suppressing the need for costly high resolution A/D converter.

2.3. System Design for high bias stability

For applications serving inertial navigation, platform stabilization and north finding, the crucial performance criteria is bias stability. Thus special system design cares have been applied to this reported accelerometer in order to optimize the bias stability performance and are reviewed here below:

- ***High stability MEMS sensor.*** Mechanical stability of the MEMS sensor is essential and drives the ultimate performance that the system can reach. At the MEMS design level, special design precautions have been taken for the positioning of the spring anchors. At the MEMS technology level, the high temperature process is essential to relax any residual stresses inside the structure. At the packaging level, it is essential to provide excellent mechanical decoupling technique. The strategy implemented is a soft die attach thus transmitting only limited stress to the accelerometer. All these design choices were essential for both short-term and long-term bias stability.
- ***Offset along the detection chain.*** Instability of the electronic offset along the detection chain will be seen by the system as an acceleration bias instability at the output. For this reason, bias stability optimization work concentrated on reducing any source of offset along the electronic amplification chain. Offsets from charge injection are a major contributor in switched capacitor circuit and are not only taken into account in the design of the switches themselves, but also in the switch addressing sequence: proper sequencing has thus been applied to avoid feeding the amplification chain with offset signal coming from charge injection. Additionally, position signal readout modulation – demodulation through a CDS (Correlated Double Sampling) sequence [9] has been applied in order to reject both offset and flickering process which is detrimental to bias stability.
- ***High stability voltage references.*** Fluctuations of the voltage reference affect the system performance through its effect during the electrostatic force phase and readout phase. Its impact is not only on the scale factor (gain or K1) but also on the bias output (K0). These fluctuations linearly affect the bias and scale factor. For this reason special design effort has been put in order to achieve a highly stable power supply, low noise and low output impedance up to high frequency.
- ***Excellent matching for electrode switching and their reproducibility.*** Significant design effort needed to be put on the design of the high voltage switches in order to keep the rise and fall times of the p-MOS and n-MOS switches (controlling the positive and negative reference voltage) to a reproducibility level in the class of tens of ppm.

3. Performance results

Measurements have been performed with a PCB testboard featuring at its heart a JLCC component package with a MEMS, an electronic circuit and a temperature sensor inside, and some servicing electronics, namely an FPGA, a crystal oscillator, power supplies and a communication module. In this demonstration phase, full characterization with a single type sensor have been performed over a sample of 11 testboards, and distribution plots will be provided for sensitive parameters.

3.1. Noise measurements

Because Sigma-Delta regulation is about rejecting quantization noise in high frequency domain through filtering (noise shaping) it is instructive to look at the noise transfer function by performing an FFT signal analysis on the 1-bit output bitstream. Figure 2 reports a typical noise transfer function of our accelerometer. White noise floor is sitting at below -120 dBg√Hz or 1 μg/√Hz in this measurement. Above 300 Hz, the combined effect of the noises of the comparator and the ADC through the digital filter becomes visible. In order to explore the lower end of the frequency spectrum, the bitstream signal is low-pass filtered through a CIC decimation filter. The resulting FFT is reproduced Figure 11. It can be seen that noise flickering starts to dominate white noise around 0.1Hz. Noise is still as low as 10 μg/√Hz at 0.01Hz.

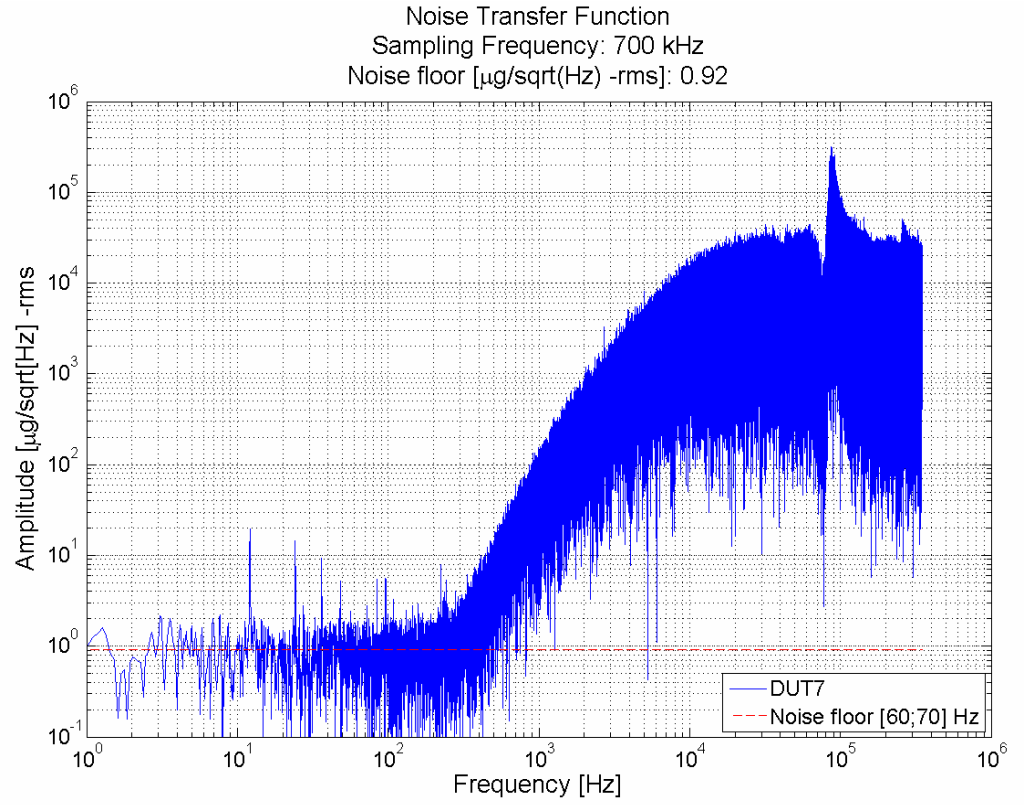

Figure 2: Typical Noise Transfer Function of Σ-Δ accelerometer

3.2. Temperature Performances

Temperature performances are evaluated over a temperature range of -40°C to +80°C, for bias (K0), scale factor (K1) and misalignment (Kp). In each case, a 3rd order polynomial curve is fitted over the parameter models (K0, K1 & Kp) and the resulting residues are extracted. The performances reported here correspond to short-term results and do not take ageing into account.

3.3. Bias stability (K0)

As mentioned in the introduction, stability of bias output is a key factor in inertial navigation and gyrocompass applications. Lots of design efforts have been put into minimizing bias stability as mentioned in paragraph 2.3, and further design work is being put on the packaging side to minimize performance degradation from assembly. The so far reached performance is already excellent with typical curves illustrated in Figure 3. Additional population data distribution is provided in Figure 4, which demonstrate that bias stability temperature slopes do not exceed 150 μg/°C and residues after 3rd order polynomial curve fitting are staying below 300 μg.

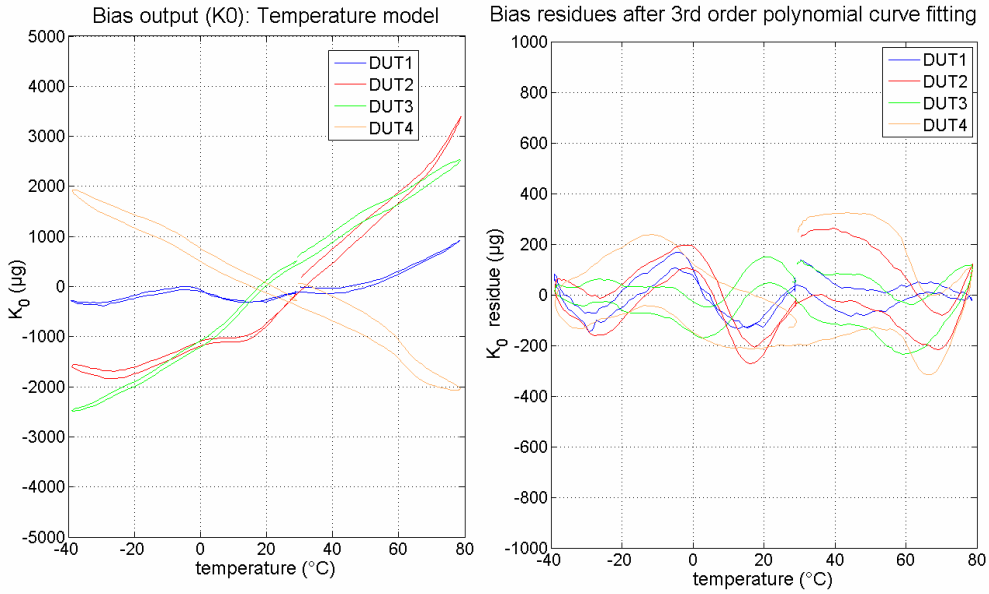

Figure 3: Bias stability (K0) performance: Temperature slopes (left) and residues (right)

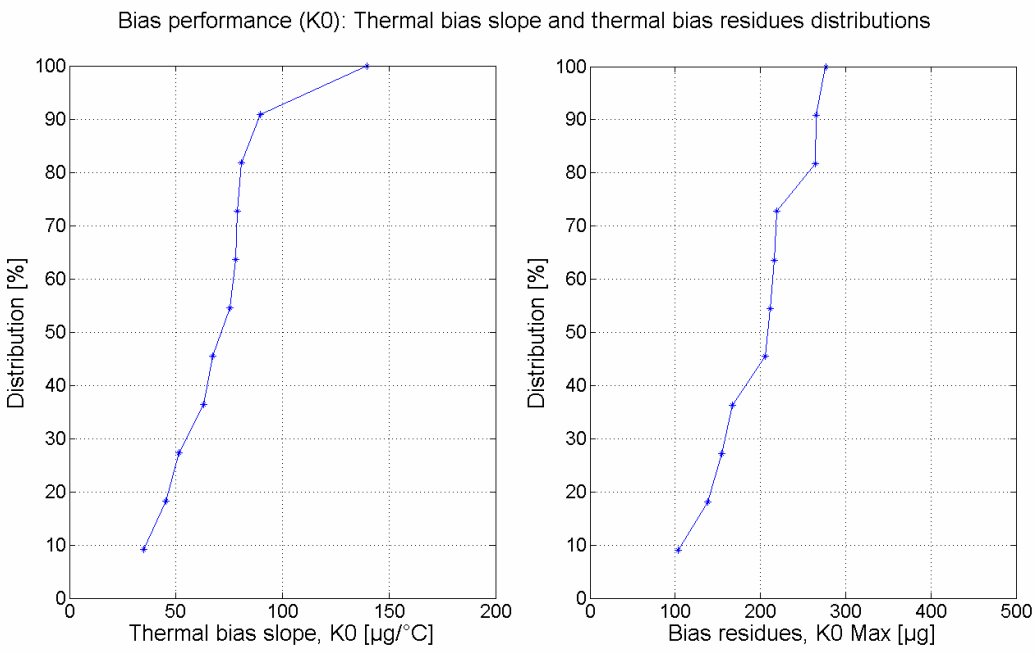

Figure 4: Bias (K0) performance: population distribution Population distribution for max thermal slope (left) and max residues (right) over the [-40 ÷ 80]°C temperature range

3.4. Scale Factor (K1)

Scale factor over temperature exhibits best class performances and excellent uniformity and repeatability from device to device with effectively 2 inflexion points as can be seen in Figure 5. Population distribution (see Figure 6) shows that scale factor temperature slope is kept well below 100 ppm/°C, while scale factor residues after 3rd order polynomial fitting stay below 200 ppm.

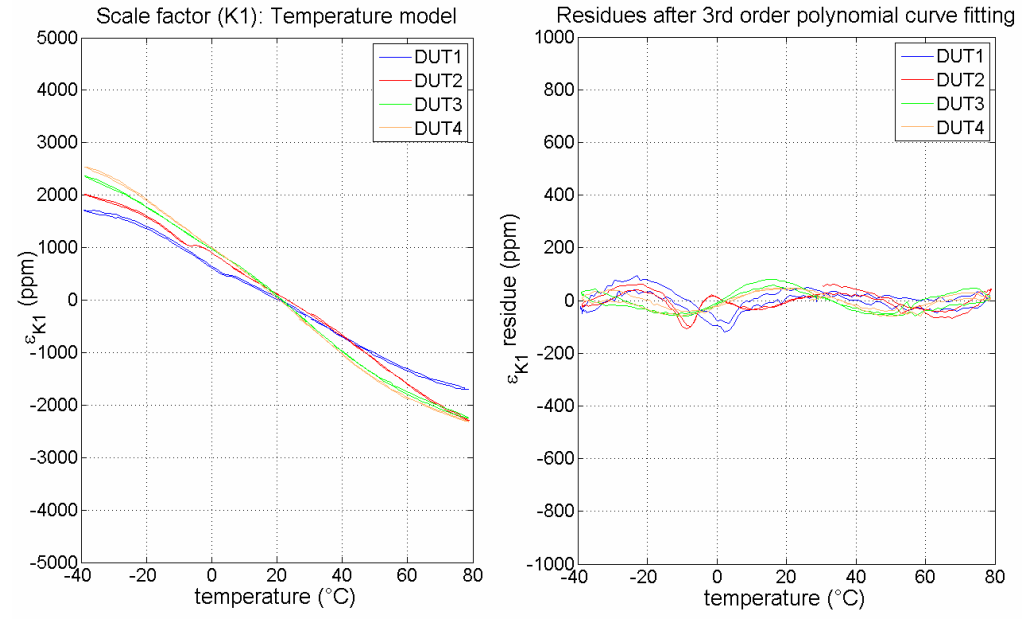

Figure 5: Scale factor (K1) performance: Temperature slope (left) and residues (right)

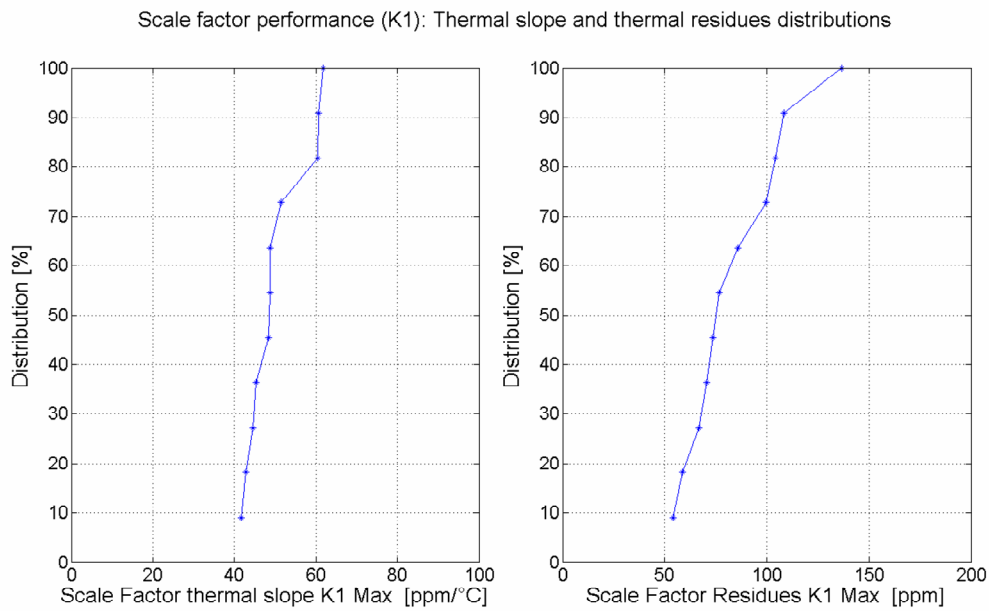

Figure 6: Scale factor (K1) performance: Population distribution for max thermal slope (left) and max residues (right) over the [-40 ÷ 80]°C temperature range

3.5. Misalignment (Kp)

Despite the fact that the demonstrators are assembled on PCB, misalignment over temperature exhibits also excellent performance as can be seen on Figure 7. Temperature slope of misalignment over the entire population is kept within 50 μrad/°C, while residues after 3rd order polynomial fitting remain below 60 μrad (see Figure 8)

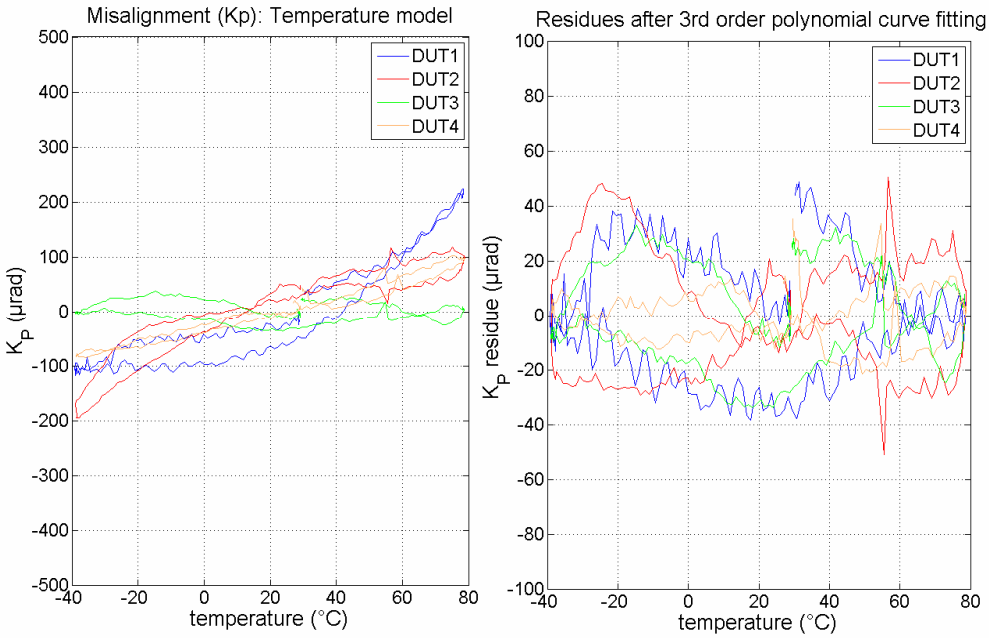

Figure 7: Misalignment (Kp) performance: Temperature slope (left) and residues (right)

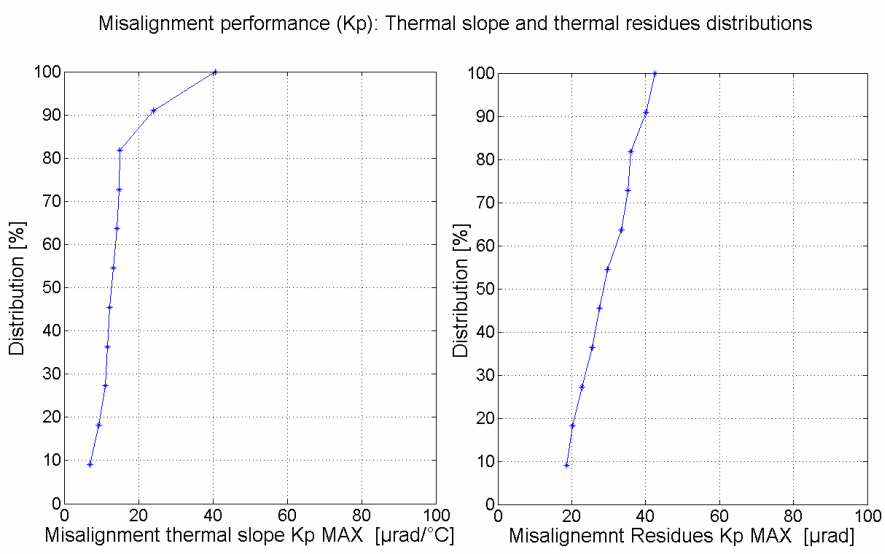

Figure 8: Misalignment (Kp) performance: Population distribution for max thermal slope (left) and max residues (right) over the [-40 ÷ 80]°C temperature range

3.6. Short-term bias stability under warm-up

In the reported curve of Figure 9, bias stability is explored under warm-up conditions, with post-data treatment introducing thermal compensation (based on the established thermal model) and doing data averaging over 1 sec. The resulting thermally compensated bias stability signal leaves only very limited warm-up transient signal. More importantly the resulting bias stability is controlled within +/-10 µg for a 15g full scale signal, which makes this accelerometer fall in the better than 1 ppm bias stability class.

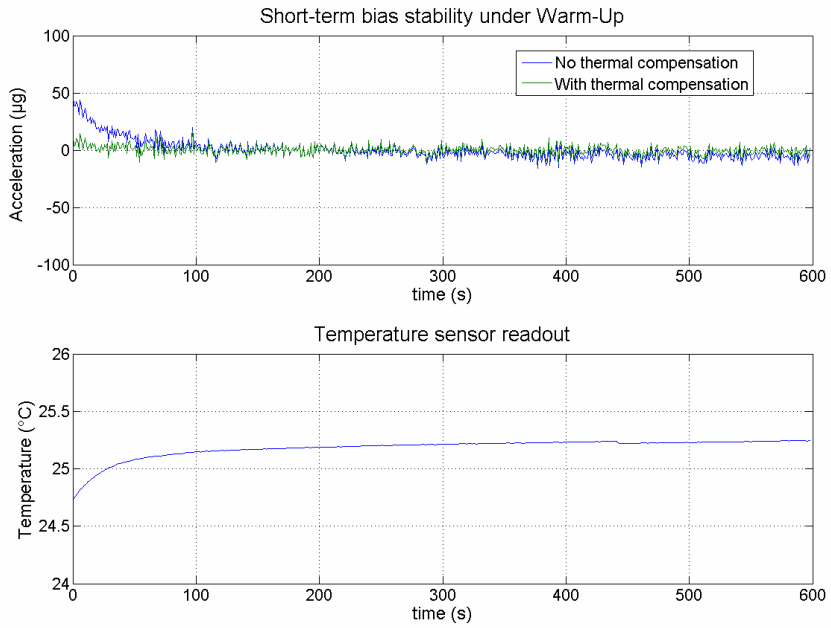

Figure 9: Warm-up test: Output acceleration, with and without temperature compensation (top) and temperature increase during test seen by MEMS and temperature sensor (bottom)

3.7. Allan Variance

One accelerometer device has been tested on longer periods in order to extract its PSD and, after averaging/decimation over 1 sec segments, its Allan Variance. The resulting plot is shown in Figure 10. It can be seen that 10 sec of data observation is required in order to access to the 1 μg signal resolution.

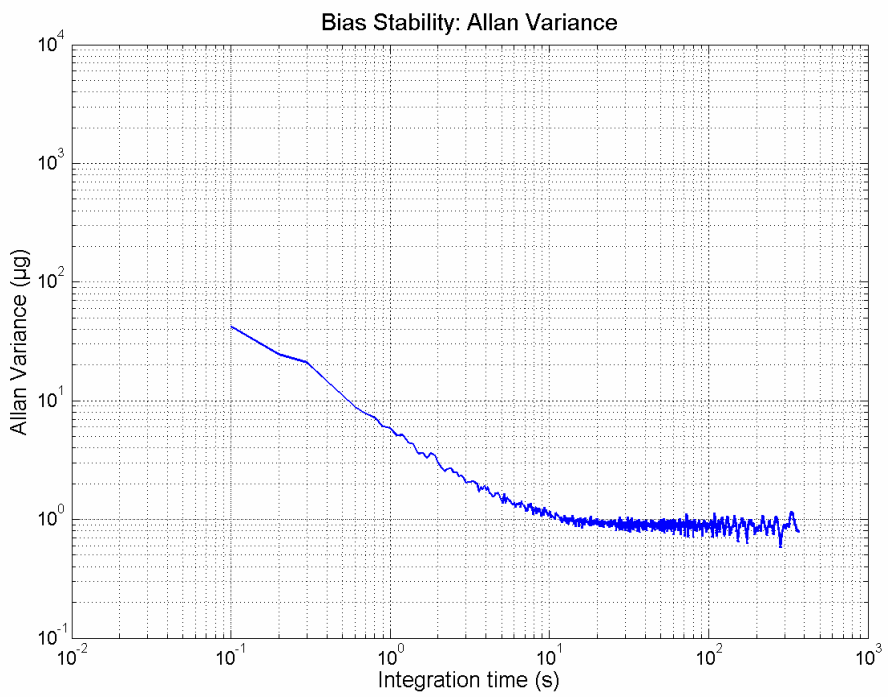

Figure 10: Allan variance plot for Σ-Δ accelerometer

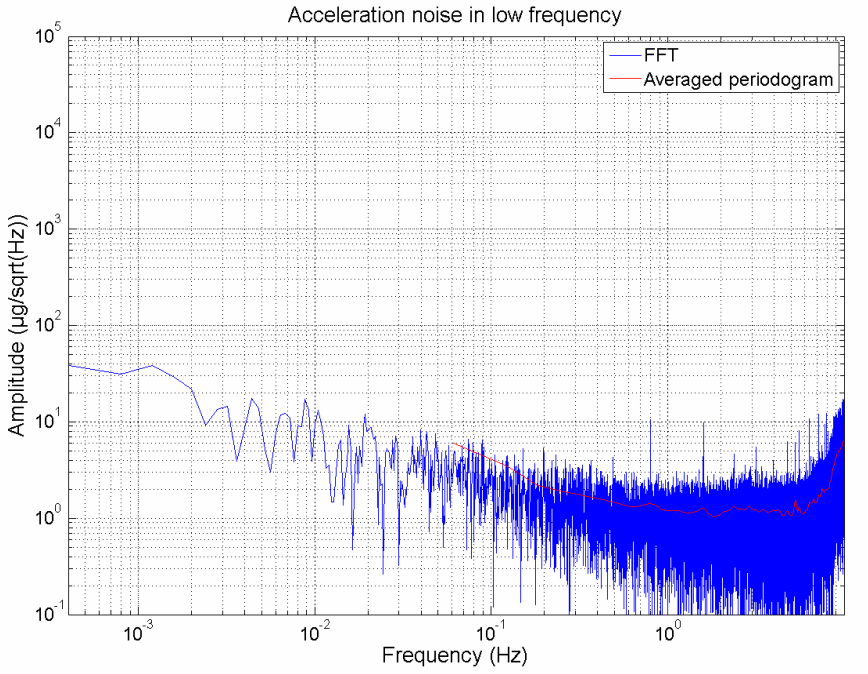

Figure 11: Same data as the ones reported in figure 9 but represented in frequency domain

The noise level (1μg/√Hz) on the PSD plot shown in Figure 11 suggests that 1 sec observation time should be enough to reach 1μg on the Allan variance. This is not the case because of the large high frequency vibration noise present in the test lab which dominates in the low time scale and explains why the -1/2 slope (corresponding to the system white noise) is not seen. The other very interesting observation is that no signal increase (i.e. drift contributions) is observed up to observation times of 300 sec.

3.8. Vibrations (K2)

Second order non-linearity (K2) is also a key parameter in inertial navigation application, especially due to the presence of significant vibrations, which through rectification, will translate into bias shift. The chosen Sigma-Delta architecture is well suited for minimizing K2 non-linearity and is confirmed through measurements presented in Fig. 9, where a sine excitation of 3g peak is being applied K2 value is kept below 10 μg/g^2 up to frequency of 200 Hz and still remains below 20 μg/g^2 up to 1 kHz. Additionally K2 curves are remarkably homogenous from device to device.

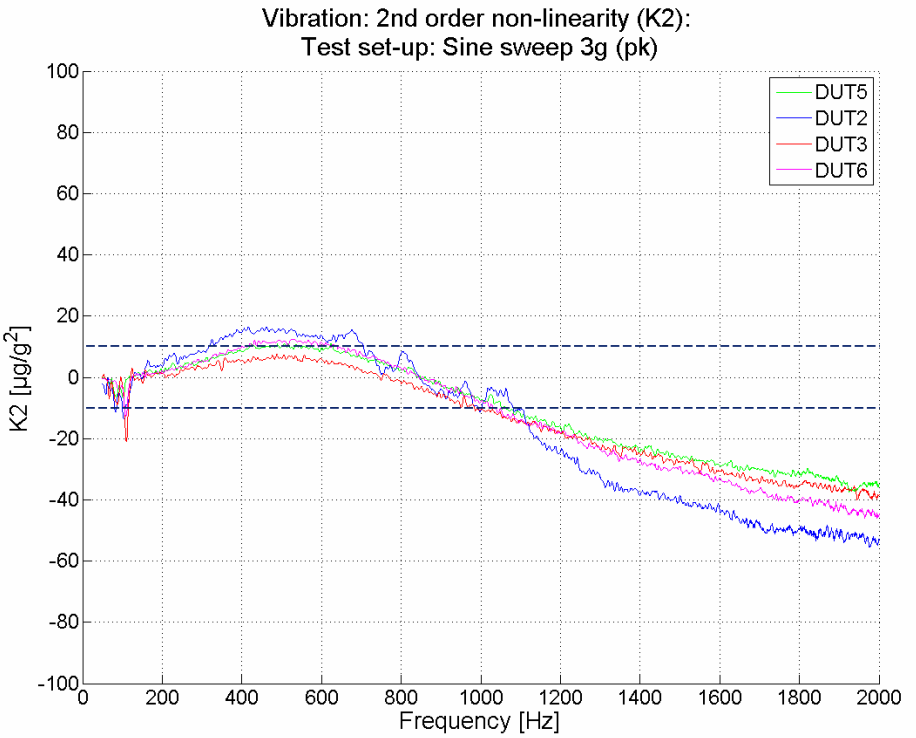

Figure 12: 2nd order non-linearity (K2) as a function of excitation frequency for a 3g peak sinusoidal input acceleration

3.9. Peformance summary

The overall accelerometer system performances in terms of max values are reviewed in table 1.

Parameters	**Performances**		
	Value	***Unit***	***Comment***
Full scale range	15	g	
Noise	2	μg/√Hz	
Bias stability (K0)			
Short-term (under warm-up)	10	μg	or 1 ppm
Temperature bias slope	150	μg/°C	
K0 Temperature residues	300	μg	
Scale factor (K1)			
K1 Temperature slope	100	ppm/°C	
K1 Temperature residues	200	ppm	
Misalignment (Kp)			
Kp Temperature slope	50	μrad/°C	
Kp Temperature residues	60	μrad	
Vibration (K2)	10 20	$\mu g/g^2$	[0; 200] Hz [200; 1000] Hz
Shock resistance	4000	g	
Power consumption	100	mW	

4. Conclusions

The accelerometer MEMS technology platform presented in this article has set a new reference for navigation grade MEMS accelerometer. Excellent scale factor stability over temperature, and good bias stability slope and residues over temperature have been reported. Further work will focus on further reducing the bias instability by improving the packaging. Further ageing characterization are also under way.

With these reported results MEMS accelerometer are now competing with the traditional macro electro-mechanical accelerometer on the market.

5. Acknowledgment

The authors would like to thank the European commission for financial support through grant CleanSky # 271492 for part of this work.

References

[1] Honeywell, Datasheet Q-Flex® Navigation Accelerometers, http://www.inertialsensor.com/inertial-navigation-accelerometers.php

[2] Innalabs, Datasheet Quartz Accelerometers INN-202/203/204/205, http://www.innalabs.com/index.php/quartz-accelerometers.html

[3] M. Lemkin and B.E. Boser, “A three-axis micromachined accelerometer with a CMOS position-sense interface and digital offset-trim electronics”, IEEE Journal of Solid-State Circuits, vol. 34, no. 4, April 1999, pp. 456-468.

[4] J.M. Tsai and G.K. Fedder, "Mechanical noise-limited CMOS-MEMS accelerometers", Technical Digest of the 18th IEEE International Conference on Micro Electro Mechanical Systems (MEMS 2005), Miami Beach, Jan.30-Feb.3, 2005, pp. 630-633.

[5] Y. Dong, P. Zwahlen, A.M. Nguyen, F. Rudolf, J.M. Stauffer, “High performance inertial grade sigma-delta MEMS accelerometer,” IEEE/ION PLANS 2010, Indian Wells, CA, May 2010, pp. 32-36.

[6] Y. Dong, P. Zwahlen, A.M. Nguyen, R. Frosio, F. Rudolf, “Ultra-high precision MEMS accelerometer,” Proceedings of Transducers, 2011 16th International, Beijing, June 2011, pp. 695-698.

[7] H. Kulah, J. Chae, N. Yazdi and K. Najafi, "Noise analysis and characterization of a sigma-delta capacitive microaccelerometer ", IEEE Journal of Solid-State Circuits, vol. 41, no. 2, Feb. 2006, pp. 352-361.

[8] M. Pastre, M. Kayal, H. Schmid, A. Huber, P. Zwahlen, A.-M. Nguyen, Y. Dong, “A 300 Hz 19b DR capacitive accelerometer based on a versatile front end in a 5th-order delta-sigma loop”, Proceedings of ESSCIRC’09, the 35th European Solid-State Circuits Conference, Athens, Greece, Sept. 14-18, 2009, pp. 288-291.

[9] C.C. Enz and G.C.Temes, “Circuit techniques for reducing the effects of op-amp imperfections: autozeroing, correlated double sampling and chopper stabilization,” Proceedings of the IEEE, vol. 84, no. 11, Nov. 1996, pp. 1584-1614.